ORGANISATION EUROPEENNE POUR LA RECHERCHE NUCLEAIRE
EUROPEAN ORGANIZATION FOR NUCLEAR RESEARCH
Laboratoire Européen pour la Physique des Particules
European Laboratory for Particle Physics

STUDY OF ENERGY DEPOSITION AND ACTIVATION FOR THE LINAC4 DUMP

L. Bruno[1], F. Cerutti[1], A. Ferrari[1], E. Mauro[2], A. Mereghetti[1], M. Silari[2]
[1]*AB/ATB,* [2]*SC/RP*

EDMS No. 973422

CERN-AB-Note-2008-047-ATB CERN-SC-2008-085-RP-TN

Abstract This document provides estimates of energy deposition and activation for the dump of the future LINAC4 accelerator. Detailed maps of power density deposited in the dump are given, allowing to perform further thermo-mechanical studies. Residual dose rates at a few cooling times for different irradiation scenarios have been calculated. Moreover, the air activation has been evaluated and doses to the reference population group and to a worker intervening in the cave at the shutdown have been predicted. Calculations were performed with the Monte Carlo particle transport and interaction code FLUKA.

CERN, 1211 Geneva 23, Switzerland
October 2008

1. Introduction

The LINAC4 [1] is a 160 MeV H^- linear accelerator, designed at CERN to replace the present 50 MeV linac (LINAC2) as injector to the Proton Synchrotron Booster (PSB). This new linac constitutes an essential component of any of the envisaged LHC upgrade scenarios and is intended to open the way to future extensions of the CERN accelerator complex towards higher performances.

The LINAC4, in its final design [2], is divided into four sections:

1 a radiofrequency quadrupole (RFQ), that firstly accelerates H^- ions up to 3 MeV;

2 a 18.7 m-long drift tube linac (DTL), up to 50 MeV;

3 a 25 m-long cell-coupled drift tube linac (CCDTL), up to 102 MeV;

4 a 22 m-long π-mode structure (PIMS), up to the final top energy of 160 MeV.

The LINAC4 line is terminated with an absorber block to collect the beam during commissioning and in the event of magnet failure [3]. The beam dump should consequently withstand the power deposited by one or more entire pulses (see Table 1). Thermal estimates were firstly made with a monolithic cylindrical dump either in graphite or in a ferritic chromium steel [4]. The present study considers a stack of equally-spaced thin metallic foils cooled by a forced air flow, proposed in order to enhance the core-to-air exchange surface.

All the accelerator components will be located in the LINAC4 tunnel, 12 m below ground level, approximately 100 m long, 4.45 m wide and 3.20 m high. The LINAC4 dump shall be situated at the intersection of the LINAC4 tunnel with the LINAC4 transfer line, after the bending magnet for beam delivery[1].

2. Simulation set up

The simulations were performed with FLUKA [5, 6] (development version FLUKA 2008). The quantities of interest[2] are the power deposition in the dump itself, the ambient dose equivalent after different cooling times, and the activities of radionuclides ejected from the LINAC4 tunnel by the ventilation system during operation, as well as those present in the dump cave at the shutdown.

[1] See drawings SPLLJL__0006 "LINAC 4 - Civil Engineering - Transfer Line to LINAC 2" and SPLLJL__0008 "LINAC 4 - Civil Engineering for Radioprotection Calculations" for further details.

[2] FLUKA results are usually normalized to primary event (i.e., primary proton) for a subsequent easy scaling by the considered beam intensity. If results are linked to a cooling time, they are instead expressed per unit time (e.g., pSv s^{-1}), since they are related to the activity induced by the provided irradiation profile.

For an accurate description of all the nuclear processes relevant for isotope production, the evaporation of heavy fragments and the coalescence mechanism were explicitly turned on via two separated `PHYSICS` cards.

The card `DEFAULTS` was used, setting defaults for precision simulations. Neutron transport below 20 MeV was performed using the multi-group approach, updated to the new 260 group library. The transport threshold for electrons/positrons and photons was 1 and 0.1 MeV, respectively, decreased by a factor of 10 for electromagnetic radiation originated by decayed nuclei at the requested cooling times.

2.1 Considered scenarios

Three scenarios have been envisaged for the LINAC4 dump irradiation (see Table 1): a 4 month *commissioning*, a "0-*cycle*" operation (planned to be of 9 months per year), and an *accident* case. This last is not relevant for activation estimates, but it is the most severe one from the point of view of thermo-mechanical stress induced in the dump by single shots.

	Scenario		
	commissioning	"0-**cycle**"	**accident**
Peak current [mA]	40	40	40
Pulse duration [μs]	50	50	400
Repetition rate [Hz]	1	1/12	1
Duty cycle [%]	0.005	$\sim$ 0.0004	0.04
Timing	4 months 12 hours per day	9 months per year 24 hours per day	2-3 shots once a month (max)
Total number of protons	**6.57 10^{19}**	**2.47 10^{19}**	**2-3 10^{14}**
Average current [protons s^{-1}]	6.25 10^{12}	1.042 10^{12}	/
Irradiation time [s]	1.0512 10^{7}	2.3652 10^{7}	/

Table 1. Summary of the LINAC4 dump irradiation scenarios considered in the present simulations. Only the commissioning and the "0-cycle" scenarios are relevant for activation estimates.

In order to evaluate residual dose rates, an irradiation profile with the commissioning scenario followed by the "0-cycle" scenario after a pause of 1 month, was implemented in FLUKA via the `IRRPROFI` card. The pulse structure of the beam was not considered, but the average current of each scenario, preserving the integrated number of impinging protons as listed in Table 1.

The residual dose rates were calculated for two different sets of cooling times, one for each considered scenario:

Commissioning scenario: at the irradiation end (actually 1 s later, in order to prevent from falling in the irradiation period due to computational accuracy), after 1 week and after 1 month (actually 100 s

before the beginning of the "0-cycle" operation for the same reason above);

"0-cycle" scenario: at the irradiation end, after 1 week, after 1 month, after 3 months and after 1 year.

2.2 The geometry model

The core of the dump is composed by a stack of 150 metallic foils, each 300 μm thick and with a 8 cm-side squared transverse section, made of a special iron alloy, whose composition is given in Table 2. The effective length is thus 4.5 cm. The foils are inter-spaced by a 3 mm gap for forced air cooling. Consequently the actual length of the dump (from the first foil to the last one, both included) is 49.2 cm. The foils were modeled through the `LATTICE` option: only a stack with the first 10 foils of the dump was implemented by scratch as prototype, whereas all other foils were replicas of such a prototype.

Element	*Weight fraction*
Al	5.0 %
Cr	22.0 %
Fe	72.8 %
Y	0.1 %
Zr	0.1 %
Density: 7.22 g cm^{-3}	

Table 2. Elemental composition and density of the Fe alloy of the foils used in the FLUKA simulations.

Element	*Weight fraction*
N	75.53 %
O	23.16 %
Ar	1.31 %
Density: 1.225 mg cm^{-3}	

Table 3. Elemental composition and density of the air used in the FLUKA simulations.

The origin of the right-handed frame of reference is placed at the cross-sectional centre of the first foil, in correspondence with its front face. The y axis is vertically oriented towards the cave roof, whereas the z axis is directed as the proton beam, starting in the simulation 1 mm upstream of the first foil. The proton energy is 160 MeV, the energy spread and the beam divergence are negligible. The beam spatial distribution, centered on the z axis, is assumed to be Gaussian both along x and y, with two different FWHMs: 0.601 cm and 1.202 cm, respectively. These two values correspond to a $r_{0.95}$ of 5 mm and 10 mm, respectively [3], being $r_{0.95}$ the distance from the distribution center within which 95 % of the particles are contained. For a Gaussian distribution, one has:

$$r_{0.95} = 1.96\sigma$$

and

$$\sigma = \frac{\mathrm{FWHM}}{2\sqrt{2\log(2)}}$$

The foils lie in an air chamber (see air composition in Table 3) the transverse section of which is 20 cm-side squared and centered on the beam axis (as the foils). Its length is 60 cm, starting 10 cm upstream of the first foil. No dump support was implemented since it had not yet been designed. Once a design will be available, simulations assessing its contribution to residual dose rates and air activation should be performed.

A 1.5 m-thick shielding made of concrete (the composition of which is given in Table 4) surrounds the air chamber. It is provided with a hole (40 mm in diameter, filled with air) to let the beam imping on the dump core. Due to its size and to the proton energy, the concrete shielding was provided with an intense biasing based on *region importance*, in order to increase particle statistics along its walls and outside.

Element	*Weight fraction*	*Element*	*Weight fraction*	*Element*	*Weight fraction*
H	0.600 %	C	5.62 %	O	49.2875 %
Na	0.453 %	Mg	0.663 %	Al	2.063 %
Si	18.867 %	K	0.656 %	Ca	20.091 %
Fe	1.118 %	P	0.048 %	S	0.012 %
Ti	0.347 %	Mn	0.0387 %	Zn	0.0241 %
Zr	0.0074 %	Ba	0.0179 %	Pb	0.0464 %
Sr	0.399 %	Eu	0.42 ppm		
Density: 2.42 g cm^{-3}					

Table 4. Elemental composition and density of the concrete of the shielding and the cave.

Figure 1 shows a 3D view of the beam dump cave as implemented in FLUKA, with the central concrete block (the dump shielding) provided with the hole for the beam (enlarged in order to be clearly visible). The yellow arrow shows the beam direction, though, as already mentioned, in the simulations the 160 MeV proton beam is assumed to start very close to the dump core, i.e. inside the air chamber. The concrete walls of the cave were implemented as well, in order to take into account the contribution of backscattered particles to ambient dose equivalent and air activation. The elemental composition is the same as for the dump shielding (see Table 4). Figure 2 shows a 3D view of the dump core in the air chamber surrounded by the concrete shielding.

3. Results

The results concerning power deposition in the dump core are shown first. Then residual dose rates are presented for a few cooling times after the two considered irradiation scenarios. The activity released into the outer atmosphere during commissioning (the most severe scenario in terms of integrated current) is calculated, together with the dose to the reference group of the population and to a worker intervening in the cave at shutdown.

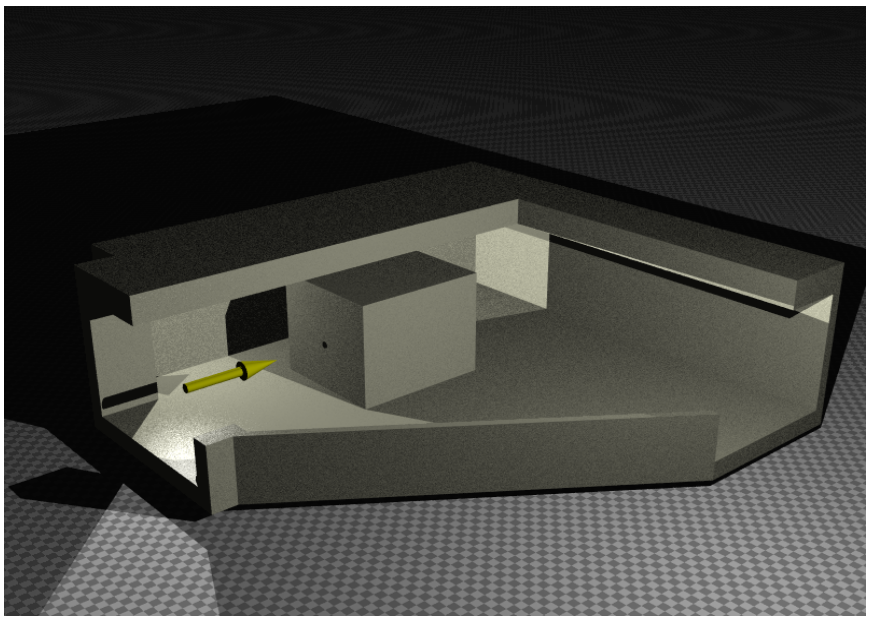

Figure 1. The LINAC4 dump cave as implemented in FLUKA, with the central concrete block for shielding the dump core. The hole for the proton beam (the axis of which is indicated by the yellow arrow) has been enlarged for being visible.

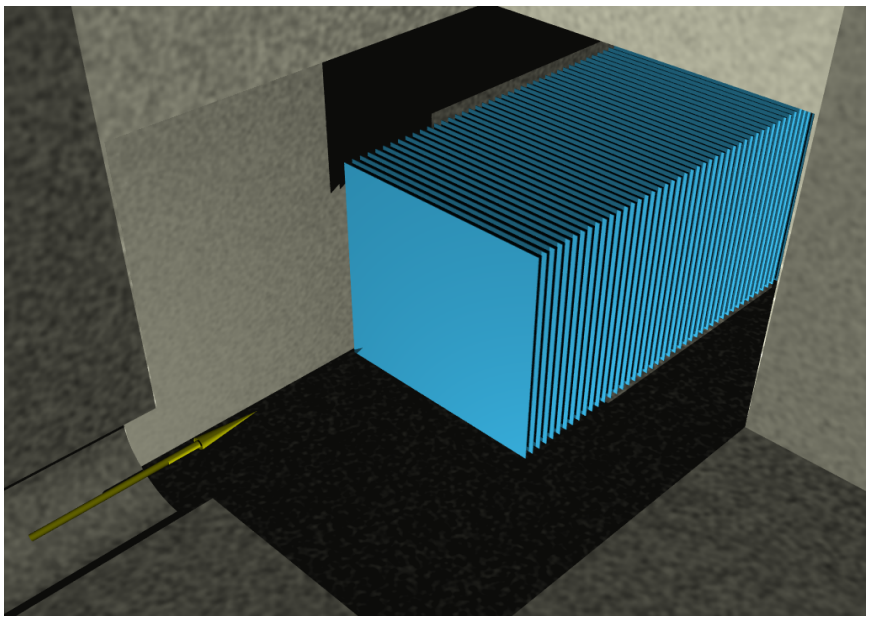

Figure 2. FLUKA implementation of the dump core consisting of a stack of air cooled thin foils placed inside a concrete shielding block. The yellow arrow indicates the axis of the beam, coming from the upstream bending magnet (when this is switched off) through the hole in the concrete.

3.1 Power deposition

The energy deposition was scored on the whole dump metal core: a cylindrical mesh, co-axial with the proton beam and covering more than the foil transverse section, was superimposed to *each* foil. The mesh has azymuthal binning of 2 degrees, radial binning of 0.5 mm and only one longitudinal bin, corresponding to the single foil length. FLUKA results are expressed in GeV cm^{-3} per primary; consequently they are converted into W cm^{-3} for the peak current of 40 mA:

$$P\left[\frac{\mathrm{W}}{\mathrm{cm}^3}\right] = E\left[\frac{\mathrm{GeV}}{\mathrm{cm}^3\ \mathrm{primary}}\right] \cdot 1.6\ 10^{-10}\frac{\mathrm{J}}{\mathrm{GeV}} \cdot \frac{40\ 10^{-3}\ \mathrm{A}}{1.6\ 10^{-19}\ \mathrm{C/primary}}$$
$$= E\left[\frac{\mathrm{GeV}}{\mathrm{cm}^3\ \mathrm{primary}}\right] \cdot 4\ 10^{7}\frac{\mathrm{J\ primary}}{\mathrm{s\ GeV}}$$

where E is the value given by FLUKA.

Figure 3 shows the profile of the peak power on the left and the integrated power on the right as a function of the depth in the dump core. The Bragg's peak is clearly visible in the plot on the right, whereas the left plot reflects the lateral propagation of the shower, which can be appreciated by comparing the two plots in Figure 4, where the power deposition maps at the peak power and at the Bragg's peak, respectively, are shown. The right plot of Figure 4 allows to evaluate the power deposition in the air around the foil, limited by the radial dimension of the adopted scoring mesh.

In case of accident, a single shot (400 μs long) deposits in the dump core a peak energy density of $\sim$ 670 J cm^{-3} and a total energy of $\sim$ 2.3 kJ. For commissioning and "0-cycle" operation (50 μs long shot), these values have to be lowered by a factor of 8. These results represent the input for possible further studies of thermo-mechanical stress induced in the foils.

3.2 Residual Dose

The residual dose rates were scored by means of a fluence detector (`USRBIN` card) with a Cartesian binning, covering all the volume inside the dump cave with bins of cubic shape and 10 cm-side. The special routine `deq99c.f` [7] was linked into the FLUKA executable in order to convert run time fluence values into ambient dose equivalent values (as invoked by the `AMB74` code in the `SDUM` of the `USRBIN` card), given in pSv s^{-1}. A dedicated detector was used for each cooling time (see Section 2.1).

3.2.1 Commissioning scenario. Figure 5 shows the residual dose rates 1 month after the end of commissioning run (see Table 1 for details about this scenario) averaged over 20 cm in the vertical direction at the beam height. As expected, the highest values outside the dump shielding are in correspondence of the hole in the concrete ("upstream" location) and of the back side of the shielding ("downstream" location). The former location is

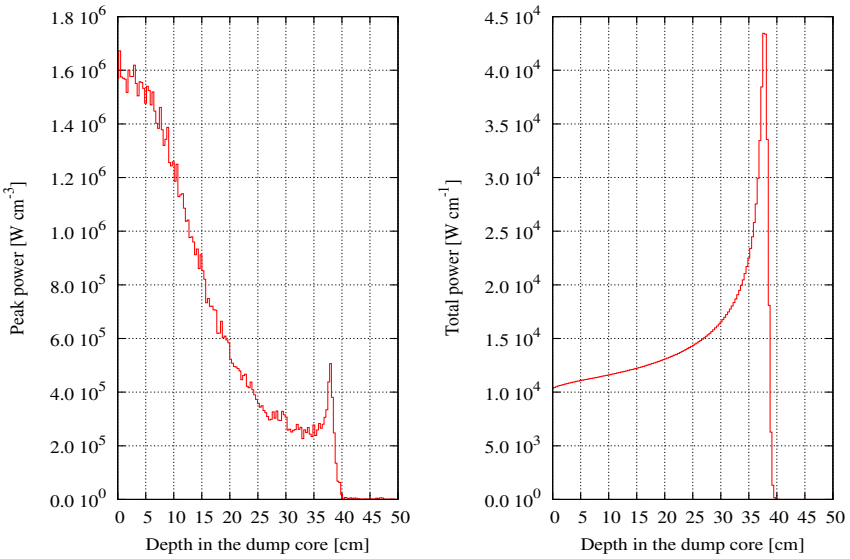

Figure 3. Profile of the peak power (left) and of the total power (right) deposited in the dump core as a function of depth in the dump. Peak power values are affected by statistical errors less than 20%, whereas the statistical error of integrated power values is much lower (<1%).

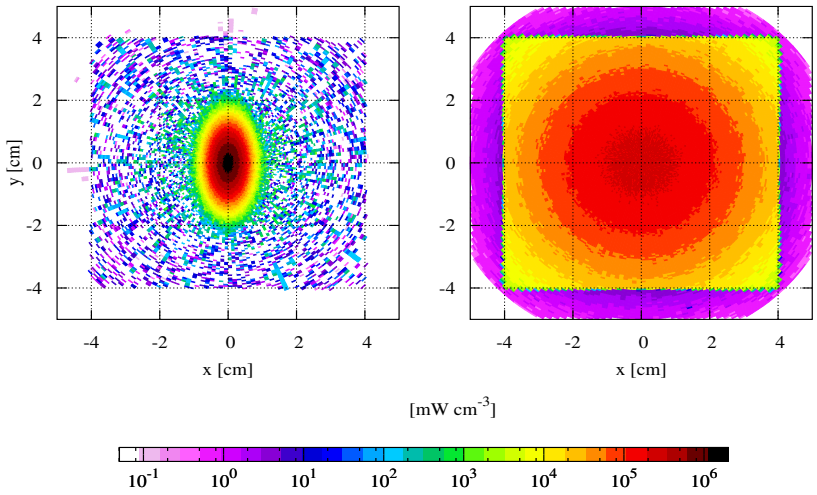

Figure 4. Power transverse distribution in the foils where the peak power (on the left - see Figure 3, left plot) and the Bragg's peak (on the right - see Figure 3, right plot) are located.

heavily affected by the radiation directly coming from the activated dump, whereas the latter is affected by the activation of the concrete shielding, showing a component of fast decaying nuclei. Table 5 shows the residual dose rates in these two locations for each cooling time.

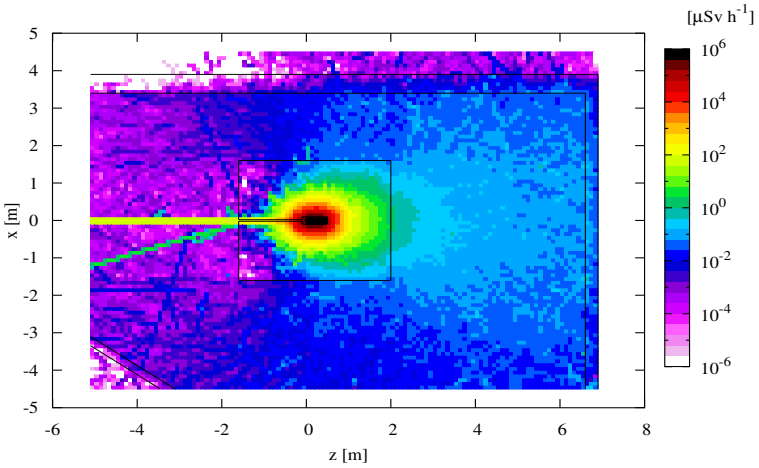

Figure 5. Residual dose rates 1 month after the commissioning end, vertically averaged over 20 cm at the beam height.

Cooling time	**Upstream location**		**Downstream location**	
	Residual dose rate [μSv h^{-1}]	*Statistical error* [%]	*Residual dose rate* [μSv h^{-1}]	*Statistical error* [%]
1 s	470	9	180	3
1 week	174	15	1.5	4
1 month	81	19	1.2	4

Table 5. Residual dose rates along the beam axis (vertically and horizontally averaged over a 20 cm side square) at the "upstream" and "downstream" locations for each cooling time after the end of commissioning.

3.2.2 "0-cycle" scenario. Figure 6 shows the residual dose rates 3 months after a "0-cycle" operation (see Table 1 for details about this scenario), averaged over 20 cm in the vertical direction at the beam height. The highest values outside the dump shielding are at the same "upstream" and "downstream" locations as before and are listed in Table 6 as a function of cooling time. Figure 7 shows the residual dose rates along the beam axis (averaged over -10 cm $< x <$ 10 cm and -10 cm $< y <$ 10 cm) for the different cooling times. It can be seen that the dose rate, downstream of the dump shielding (where it is dominated by the residual activity of the concrete), has a very significant decrease already one week after the shutdown, and then it remains almost stable. On the contrary, where it is dominated by the residual activity in the dump core, its decrease with the cooling time is more regular.

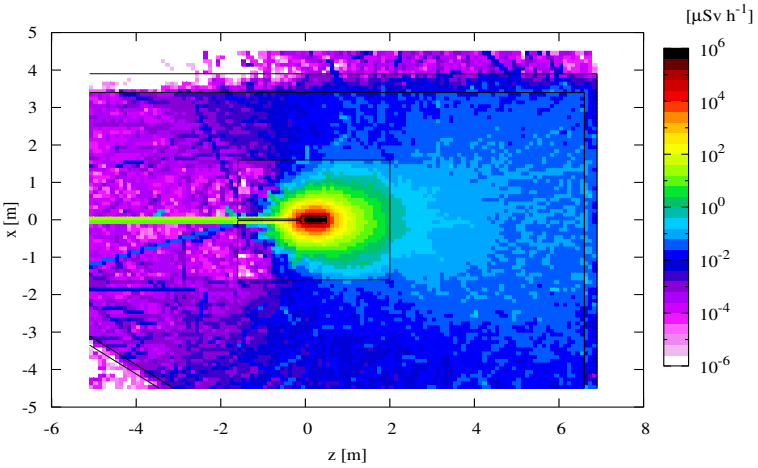

Figure 6. Residual dose rates 3 month after a "0-cycle" operation vertically averaged over 20 cm at the beam height.

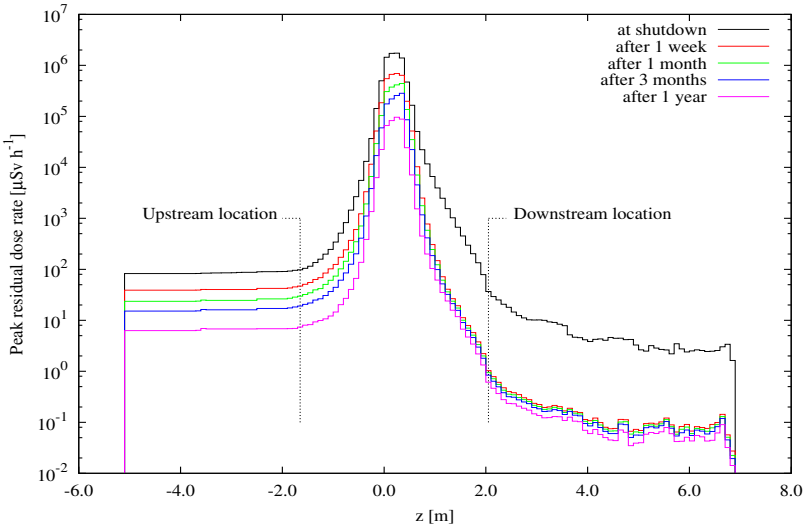

Figure 7. Residual dose rates along the beam axis (vertically and horizontally averaged over a 20 cm side square) for the considered cooling times after the end of a "0-cycle" operation. The dashed lines indicate the shielding limits.

Cooling time	**Upstream location**		**Downstream location**	
	Residual dose rates [μSv h^{-1}]	*Statistical error* [%]	*Residual dose rates* [μSv h^{-1}]	*Statistical error* [%]
0 s	98	10	37	3
1 week	47	15	1.0	4
1 month	29	17	0.9	4
3 months	19	18	0.8	4
1 year	7	23	0.6	4

Table 6. Residual dose rates along the beam axis (vertically and horizontally averaged over a 20 cm side square) at the "upstream" and "downstream" locations for each cooling time after a "0-cycle" operation.

3.3 Air activation

Due to the very low interaction probability of particles in air, the calculation of air activation had to be carried out in two steps. The energy distribution of hadron fluence in air was scored run time, and folded afterwards with the cross sections for radioisotope production on the target nuclei in the air compound. A dedicated set of track-length estimators was implemented in the FLUKA input file for each of the three regions containing air (the region surrounding the dump foils inside the concrete shield, the hole in the concrete shield, and the region surrounding the concrete shield). Such estimators are represented by `USRTRACK` cards for protons and neutrons. Most of the scored track-length is obviously located in the region inside the concrete shield, though it represents only less than 10^{-4} of the irradiated volume, corresponding to the union of the three mentioned geometry regions (about 360 m^3). As a consequence, the presence of the dump support could in principle impact the track-length spectrum and thus its effect should be checked through future simulations.

The activity of a radioisotope in the dump cave at the end of the irradiation period T is given by

$$A_T = A_S \left(1 - \exp\left(-(\lambda + m_{on})T\right)\right) \tag{1}$$

where λ is the decay probability per unit time and m_{on} is the relative air exchange rate during irradiation, giving the fraction of the total air volume renewed per unit time. We assume that the ventilation system of the LINAC4 tunnel provides a recycling of 1000 m^3 per hour out of a total air volume of 1800 m^3. A_S is the saturation activity [8]:

$$A_S = \frac{V\lambda}{\lambda + m_{on}} \sum_{P,T,j} \phi_P(E_j)\sigma_{P,T}(E_j)N_T\left(\Delta E\right)_{j,P} \tag{2}$$

where the sum has to be performed over the produced hadron species P (just protons and neutrons in our case), the target nuclear species T in air (^{12}C, ^{14}N, ^{16}O, and ^{40}Ar), and all the bins j into which the hadron energy range has been divided. V is the irradiated air volume, ϕ is the differential fluence rate (given by FLUKA in cm^{-2} GeV^{-1} per primary and to be scaled by the average proton current), σ is the production cross section for the considered radioisotope[3], and N_T is the number of target nuclei per unit volume, calculated from the detailed air composition given in Table 7. Table 8 (fifth column) lists the residual activity A_T of the radioactive species present in the air at the end of commissioning.

For each radioisotope, the total amount of activity released into atmosphere all along the irradiation period T is

$$A_{on} = m_{on}A_S\left(T - \frac{1 - \exp\left(-(\lambda + m_{on})T\right)}{\lambda + m_{on}}\right)\exp\left(-\lambda\ t_{on}\right) \tag{3}$$

[3]The cross section values were partly taken from [9] and partly computed by FLUKA.

Molecule	*Weight fraction* [%]	*Atomic mass* [g mol^{-1}]
CO_2	0.05	44.0
N_2	75.52	28.0
O_2	23.15	32.0
Ar	1.29	40.0
Density: 1.205 mg cm^{-3}		

Table 7. Air composition used in the post-processing calculation of air activation.

where t_{on} is the time taken by the air flux ro reach the release point from the irradiated area where air is being activated. In our case t_{on} is assumed to be equal to 150 s. Table 8 (third column) gives the total activity A_{on} ejected into the external air over the 4 month commissioning.

Finally, the total amount of activity released into the atmosphere *after* shutdown, can be obtained by the expression

$$A_{off} = A_T \frac{m_{off}}{\lambda + m_{off}} \exp\left(-\lambda\ t_{off}\right) \tag{4}$$

with m_{off} and t_{off} representing the same quantities as m_{on} and t_{on}, respectively, but referred to the period following the irradiation end.

3.4 Dose to the reference group of the population and to a worker intervening in the cave at the shutdown

The environmental impact of an accelerator facility must be assessed in terms of radioactivity released in the environment and in terms of effective dose to the reference group of the population. As a complete description of the environment is not achievable and the population behavior cannot be predicted, a conservative approach must be employed. In general the so-called screening approach is used [10]: it makes use of simplified models that overestimate the activity densities and the effective doses. When assessing the impact of air releases from the stacks, both diffusion due to the winds and deposition in environmental matrices must be considered. For the external exposure, the effective dose must be integrated over one year. For the internal exposure, the effective dose committed during the rest of life due to inhalation and/or ingestion of radioactive substances in one year shall be evaluated. All these factors have been considered in a previous study [11] and the resulting conversion coefficients from activity to effective dose, expressed in Sv/Bq, calculated for the existing ISOLDE stack were here employed. They are based on the Swiss directive HSK-R-41 [12] and they apply to the most exposed group of the population, which consists of the border guards and their families working at the Swiss border guard station on the Route de Meyrin and living in adjacent houses. The activity released to the external air over 4 months of commissioning was converted, through these coefficients, to effective dose. This approximation

Radio-isotope	λ [s^{-1}]	*Activity released into atmosphere* [*Bq*]	*Dose to the population* [μSv]	*Residual activity* [*Bq*]	*Dose rate for internal exposure* [$\mu Sv\ h^{-1}$]
^{3}H	1.8 10^{-9}	1.0 10^{6}	7.79 10^{-8}	6.3 10^{2}	1.72 10^{-5}
^{7}Be	1.5 10^{-7}	1.4 10^{8}	**4.27 10^{-3}**	8.5 10^{4}	**2.61 10^{-3}**
^{10}Be	1.5 10^{-14}	1.2 10^{0}	2.36 10^{-10}	7.7 10^{-4}	9.75 10^{-9}
^{11}C	5.7 10^{-4}	1.7 10^{11}	**3.98 10^{-2}**	1.1 10^{8}	2.35 10^{-1}
^{14}C	3.8 10^{-12}	3.1 10^{4}	3.78 10^{-7}	1.9 10^{1}	7.35 10^{-6}
^{13}N	1.2 10^{-3}	2.7 10^{11}	**5.05 10^{-2}**	2.0 10^{8}	
^{18}F	1.1 10^{-4}	3.4 10^{7}	4.52 10^{-5}	2.1 10^{4}	**1.30 10^{-3}**
^{22}Na	8.4 10^{-9}	4.8 10^{2}	6.19 10^{-6}	3.0 10^{-1}	4.00 10^{-7}
^{24}Na	1.3 10^{-5}	1.3 10^{6}	3.72 10^{-5}	8.2 10^{2}	2.90 10^{-4}
^{27}Mg	1.2 10^{-3}	4.0 10^{6}	8.76 10^{-6}	2.9 10^{3}	
^{28}Mg	9.2 10^{-6}	3.4 10^{5}	8.36 10^{-6}	2.1 10^{2}	2.38 10^{-4}
^{26}Al	3.0 10^{-14}	1.4 10^{-3}	2.14 10^{-10}	8.6 10^{-7}	8.03 10^{-12}
^{31}Si	7.3 10^{-5}	9.9 10^{6}	4.14 10^{-6}	6.2 10^{3}	4.55 10^{-4}
^{32}Si	1.3 10^{-10}	1.9 10^{1}	7.05 10^{-9}	1.2 10^{-2}	4.40 10^{-7}
^{32}P	5.6 10^{-7}	3.4 10^{6}	2.59 10^{-4}	2.1 10^{3}	**4.06 10^{-3}**
^{33}P	3.2 10^{-7}	1.4 10^{6}	1.62 10^{-5}	8.8 10^{2}	7.63 10^{-4}
^{35}S	9.2 10^{-8}	4.5 10^{5}	4.59 10^{-6}	2.8 10^{2}	2.24 10^{-5}
^{38}S	6.8 10^{-5}	1.3 10^{7}	3.33 10^{-5}	8.1 10^{3}	
^{36}Cl	7.3 10^{-14}	2.0 10^{0}	2.18 10^{-8}	1.2 10^{-3}	4.08 10^{-9}
^{38}Cl	3.1 10^{-4}	7.0 10^{8}	6.16 10^{-4}	4.5 10^{5}	**2.19 10^{-2}**
^{39}Cl	2.1 10^{-4}	8.1 10^{8}	8.99 10^{-4}	5.2 10^{5}	**2.63 10^{-2}**
^{37}Ar	2.3 10^{-7}	6.6 10^{6}	1.33 10^{-12}	4.1 10^{3}	
^{39}Ar	8.2 10^{-11}	5.2 10^{3}	3.96 10^{-12}	3.2 10^{0}	
^{41}Ar	1.1 10^{-4}	9.7 10^{8}	3.60 10^{-4}	6.1 10^{5}	
^{38}K	1.5 10^{-3}	2.3 10^{8}	2.76 10^{-4}	1.7 10^{5}	
^{40}K	1.7 10^{-17}	1.5 10^{-4}	3.20 10^{-12}	9.3 10^{-8}	1.86 10^{-13}
^{14}O	9.8 10^{-3}	1.2 10^{10}	1.42 10^{-3}	3.2 10^{7}	
^{15}O	5.7 10^{-3}	1.1 10^{11}	**7.63 10^{-3}**	1.5 10^{8}	
^{19}O	2.6 10^{-2}	6.8 10^{2}	8.84 10^{-12}	2.0 10^{1}	
^{28}Al	5.2 10^{-3}	2.0 10^{7}	5.56 10^{-5}	2.7 10^{4}	**3.06 10^{-2}**
^{29}Al	1.8 10^{-3}	1.5 10^{7}	3.83 10^{-6}	1.2 10^{4}	
^{34}Cl	4.5 10^{-1}	1.7 10^{-22}	1.73 10^{-34}	4.0 10^{4}	
^{40}Cl	8.6 10^{-3}	1.7 10^{7}	2.96 10^{-6}	3.7 10^{4}	
^{25}Na	1.2 10^{-2}	2.8 10^{5}	4.54 10^{-9}	1.0 10^{3}	
^{23}Ne	1.9 10^{-2}	2.5 10^{4}	1.11 10^{-10}	2.5 10^{2}	
^{24}Ne	3.4 10^{-3}	2.2 10^{4}	1.21 10^{-9}	2.2 10^{1}	
^{30}P	4.6 10^{-3}	7.4 10^{6}	1.35 10^{-6}	9.2 10^{3}	
^{35}P	1.5 10^{-2}	4.1 10^{6}	1.74 10^{-5}	2.3 10^{4}	
^{37}S	2.3 10^{-3}	5.2 10^{7}	2.04 10^{-5}	4.5 10^{4}	
Sum		**5.65 10^{11}**	**1.06 10^{-1}**	**4.94 10^{8}**	**3.23 10^{-1}**

Table 8. Total activity released into the atmosphere over 4 months of commissioning (third column) and corresponding dose for exposure to the reference group of the population (fourth column); residual activity in air of the dump cave at shutdown after 4 months of commissioning (fifth column) and corresponding dose inhaled by a worker intervening in the LINAC4 tunnel at that time (sixth column). The contributions of the most important radioisotopes are highlighted in bold.

is conservative because the LINAC4 building will be further away from the guard station with respect to the ISOLDE building. The dose conversion

coefficients for adults in Table 1 of ref. [11] were used and the dose to the reference group of the population is listed in Table 8 (fourth column). The most important radionuclides contributing to the dose are ^{11}C and ^{13}N and the total dose is 0.106 μSv.

The residual activity in the cave after 4 months of run was used to estimate the dose received by worker intervening in the cave after the shutdown. If the activity is mixed homogeneously in the tunnel, the activity concentration is obtained by dividing the activity by the volume of air. To estimate the inhalation dose it is necessary to multiply the activity concentration by the breathing rate B_r and the inhalation activity-to-dose conversion factors e_{inh} (expressed in Sv Bq^{-1}), which were taken from the Swiss ordonnance [13].

The standard breathing rate for a worker is 1.2 m^3 h^{-1} and the volume of air considered is 1800 m^3. The inhalation dose is shown in Table 8. The most important radionuclides contributing to the inhaled dose are ^{28}Al, ^{38}Cl and ^{39}Cl and the total inhalation dose is 0.323 μSv per hour of exposure time.

4. Conclusions

Simulations for calculating the power deposition in the LINAC4 dump were carried out, and detailed maps are available for further thermo – mechanical studies. The estimated peak energy deposition per shot is roughly 670 J cm^{-3}, whereas the total energy deposited per shot is 2.3 kJ.

3D maps of residual dose rates have been calculated for different irradiation scenarios and cooling times. The hottest locations outside the dump shielding are in correspondence with the hole for the beam entrance and along the beam axis on the opposite downstream side, being the residual dose rates of 470 and 180 μSv h^{-1}, respectively, at shutdown after 4 months of commissioning and 98 and 37 μSv h^{-1}, respectively, at shutdown after a "0-cycle" operation.

The total activity released into the atmosphere all along the commissioning period together with the residual activity in the dump cave after commissioning is given. This information is used to calculate the dose received by the reference group of the population and by a worker intervening in the LINAC4 tunnel just after shutdown.

Acknowledgments

The authors wish to thank A. Lombardi, S. Maury, and M. Vretenar for essential and valuable input information, and M. Brugger for very useful discussions.

References

[1] L. Arnaudon et al, "LINAC4 Technical Design Report", M. Vretenar and F. Gerick, Editors, CERN-2006-AB-084 (2006);

[2] M. Vretenar et all: "Status of the LINAC4 Project at CERN", to be published

[3] "The 160 MeV Beam Dump of LINAC-4 - Functional Specification", 27^{th} August 2007, EDMS Doc. No. 871833;

[4] "The 160 MeV Beam Dump of LINAC-4 - Technical Specification", 15^{th} May 2008, EDMS Doc. No. 879980;

[5] A. Ferrari, P.R. Sala, A. Fassò, and J. Ranft: "FLUKA: a multi-particle transport code", CERN-2005-10 (2005), INFN/TC_0511, SLAC-R-773;

[6] G. Battistoni, S. Muraro, P.R. Sala, F. Cerutti, A. Ferrari, S. Roesler, A. Fassò, J. Ranft: "The FLUKA code: Description and benchmarking", Proceedings of the Hadronic Shower Simulation Workshop 2006, Fermilab 6–8 September 2006, M. Albrow, R. Raja eds., AIP Conference Proceeding 896, 31-49 (2007);

[7] S. Roesler and G. Stevenson: "deq99.f - A FLUKA user-routine converting fluence into effective dose and ambient dose equivalent", Technical Note CERN-SC-2006-070-RP-TN, EDMS Document No. 809389 (2006);

[8] C. Birattari, M. Bonardi, A. Ferrari, M. Silari: "Neutron Activation of Air by a Biomedical Cyclotron and an Assessment of Dose to Neighbourhood Populations", in Rad. Prot. Dos., Vol. 14 (1986), Issue 4, 311-319;

[9] M. Huhtinen: "Determination of Cross Sections for Assessments of Air Activation at LHC", Technical Memorandum CERN/TIS-RP/TM/96-29 (1997);

[10] P. Vojtyla: "Models for Assessment of the Environmental Impact of Radioactive Releases from CERN Facilities", CERN-SC-2005-005-IE;

[11] P. Vojtyla: "Dose Conversion Coefficients for Exposure of the Reference Population Group to Radionuclides in Air Released from the ISOLDE Facility", CERN-SC-2008-001-IE-TN (2008);

[12] Hauptabteilung fur die Sicherheit der Kernanlagen (HSK): "Berechnung der Strahlenexposition in der Umgebung aufgrund von Emissionen radioaktiver Stoffe aus Kernanlagen", HSK-R-41/d (July 1997);

[13] "Swiss Legislation on Radiological Protection (Ordonnance sur la Radioprotection)", ORaP of 22^{nd} June 1994 (state 4^{th} April 2000).